Chapter 8

The Vicsek Model

Collective dynamics often emerge in living systems: Fishes swim in schools, migrating birds fly in flocks, herds of cattle move together during seasonal migration, bees fly in swarms. Even microorganisms like bacteria sometimes swarm. And also the motion of human crowds exhibits collective dynamics. Swarming-like behaviors are instinctive in simpler species. In more complex species, they might result from conscious individual decisions. Often a collective behavior entails some distinctive advantage both for the individuals and for the group. Moving in flocks, schools, and herds benefits the individuals by providing more protection against predators (Fig. 8.1), or by reducing the energy cost of locomotion. Mutual coordination and cooperation between individuals allow a group to have better chances of survival, for example in harsh natural environments, preserving heat, energy, protecting offspring, deterring predators, and optimizing foraging.

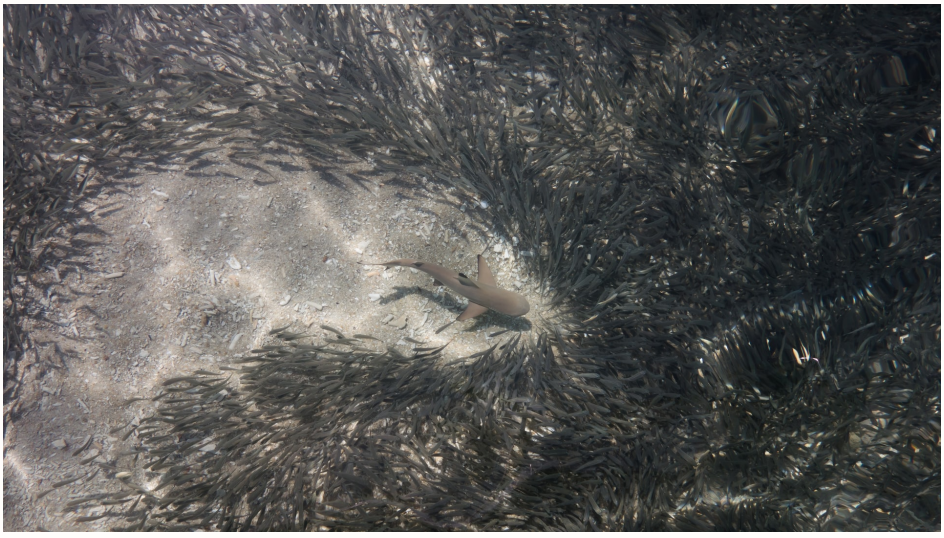

Figure 8.1: **Living organisms self-organize.** In Nature, we find several examples of self-organized living systems. Collective dynamics provide advantages for the species adopting it, for example, by increasing the chances of an individual to escape a predator, as in this photograph. *Source: Photo by Kris Mikael Krister on Unsplash under Unsplash License.*

Understanding the mechanisms determining the emergence of collective motion and leading to swarm-like behavior is of utmost importance in biology and ethology, but has also applications in technology, e.g., in the realization of robotic swarms for search-and-rescue operations, or targeted collection and delivery, in biotechnology and medical engineering, to contain or eradicate the spreading of pathogens and biological pests, and also in computer graphics, for a realistic rendering of animal or crowd behavior. So, how do collective motion and swarm-like behaviors emerge in social organisms? How does the individual determine its motion on the basis of the local sensory information about other individuals in its surroundings?

The *Vicsek model* is a minimalist model that accounts for swarm-like behavior [1]. The model itself is based on a very simple interaction rule: The individual, which moves at a constant speed, keeps on adjusting its direction to match the average direction of its neighbors. The Vicsek model has a second-order phase transition to a kinetic, swarm-like phase, upon approaching a critical value of the noise parameter. Varying the noise level in the system, the density of the individuals, and the individual radius, the Vicsek model switches from a gas-like phase, where the individuals move almost independently from each other, to a swarming phase, where individuals self-organize in clusters.

In this chapter, we start from the standard definition of the Vicsek model, showing how the different phases emerge as a function of the individual speed, interaction radius, noise level, and density of individuals. Then, we explore a few variations of the model, from slightly different rules for the individuals to calculate their orientation to the effect of delay in elaborating the sensory information from the surrounding individuals.

Example codes: Example Python scripts related to this chapter can be found on:
https://github.com/softmatterlab/SOCS/tree/main/Chapter%5F08%5FVicsek%5FModel
Readers are welcome to participate in the discussions related to this chapter on:
https://github.com/softmatterlab/SOCS/discussions/17

8.1 The standard Vicsek model

In the following, we will refer to each individual as a *particle* (sometimes they are also called *agents*). All the N particles in the system are point-like and have the same *propulsion speed* v. The two-dimensional arena where the particles move is a square of side L centered at the origin of the axes, taken with *periodic boundary conditions*: When a particle crosses over the right boundary at $x = \frac{L}{2}$, then it re-enters from the left; and something analogous happens in the case the particle crosses any of the arena boundaries, as per the following rules:

$$\begin{cases} x \to x+L & \text{if} \quad x < -\frac{L}{2} \\ x \to x & \text{if} \quad -\frac{L}{2} \le x \le \frac{L}{2} \\ x \to x-L & \text{if} \quad x > \frac{L}{2} \end{cases} \qquad \begin{cases} y \to y+L & \text{if} \quad y < -\frac{L}{2} \\ y \to y & \text{if} \quad -\frac{L}{2} \le y \le \frac{L}{2} \\ y \to y-L & \text{if} \quad y > \frac{L}{2} \end{cases} \tag{8.1}$$

Each particle interacts with all the other particles within a given distance R_{f}, called the *flocking radius*. Because of the periodic boundary conditions, each particle might also interact with particles located on the opposite side of the arena, as shown in Fig. 8.2. At time step

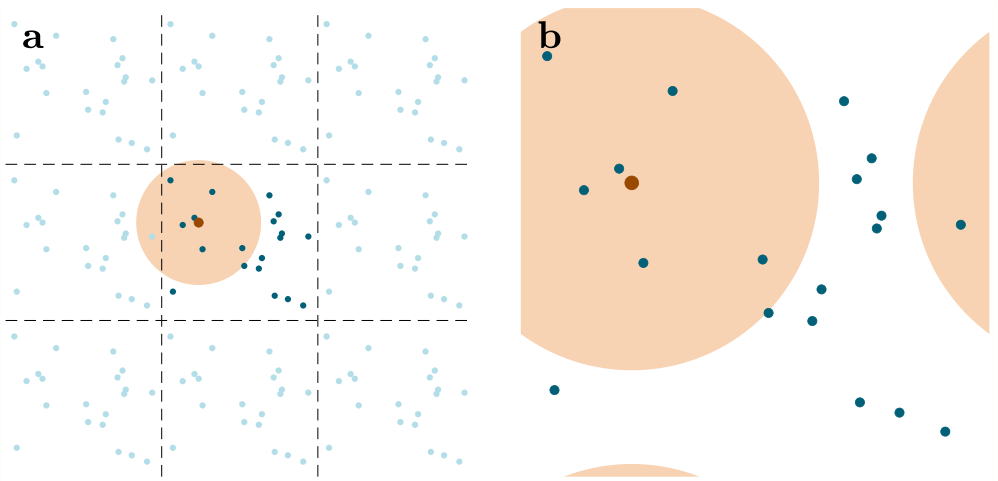

Figure 8.2: **Two-dimensional arena with periodic boundary conditions. a** A representation of the particles (full-color cyan dots) and their replicas (semi-transparent cyan dots) in the *unfolded* arena. For a given particle in the arena (larger red particle), the interaction area (or flocking area) is represented by the orange region. **b** The interaction area *folded* on the main arena. The large red particle (which is at the center of the interaction area) interacts also with a particle on the other side of the arena.

$t_n = n\Delta t$, particle j has position $\mathbf{r}_{j,n} = (x_{j,n}, y_{j,n})$ and orientation $\theta_{j,n}$. This means that the particle is moving with a velocity vector given by $\mathbf{v}_{j,n} = (v\cos\theta_{j,n}, v\sin\theta_{j,n})$. At each time step n, each particle collects information from all the particles in its flocking area and adjusts its orientation at the following time step $n+1$ according to

$$\theta_{j,n+1} = \langle \theta_{k,n} \rangle + \eta W_n \Delta t, \tag{8.2}$$

where η is the *noise* and W_n are a random number with a Gaussian distribution with mean $\mu = 0$ and standard deviation $\sigma = 1$, and the average is calculated on the particles within the flocking radius only, i.e., indexed by k with the condition $\left|\mathbf{r}_{k,n} - \mathbf{r}_{j,n}\right| < R_\mathrm{f}$ (the particle j itself is included in the averaging). The velocity at time step t_{n+1} is then calculated as

$$\mathbf{v}_{j,n+1} = v\left(\cos\theta_{j,n+1}\,\hat{\mathbf{x}} + \sin\theta_{j,n+1}\,\hat{\mathbf{y}}\right) \tag{8.3}$$

and the position as

$$\mathbf{r}_{j,n+1} = \mathbf{r}_{j,n} + \mathbf{v}_{j,n+1}\,\Delta t. \tag{8.4}$$

Therefore, only four parameters determine the behavior of the Vicsek model (excluding finite-size effects): the speed v, the flocking radius R_f, the particle density $\rho = \frac{N}{L^2}$, and the noise level η.

Exercise 8.1: Periodic boundary conditions. This first exercise is about implementing the correct functions for the motion in an arena with periodic boundary conditions. Our system is made by N point-like particles in a square arena with side L. The interaction radius is R_f.

a. Generate a set of N random positions $\mathbf{r}_j$, with $j \in \{1,2,...N\}$ within the square arena. Displace all the particles by a small vector $\Delta\mathbf{r} = \Delta x\,\hat{\mathbf{x}} + \Delta y\,\hat{\mathbf{y}}$. Write a function that, given the new displaced position $\mathbf{r}'_j = \mathbf{r}_j + \Delta\mathbf{r}$, calculates the new correct position within the arena, implementing the periodic boundary conditions stated in Eq. 8.1.

b. Implement a function that, given the positions of N particles in a square arena with side L, determines all the particles within a distance R_f from a given particle j with position $\mathbf{r}_j$, taking into account the periodic boundary conditions, as represented in Fig. 8.2b.

To monitor the global alignment of the system as time evolves, we define the *global alignment coefficient*:

$$\psi_n = \frac{1}{N}\left|\sum_{j=1}^{N}\frac{\mathbf{v}_{j,n}}{v}\right|, \tag{8.5}$$

which takes values in the interval $[0, 1]$. Values close to 0 indicate the lack of any orientational order, while values close to 1 are an indication of a phase with high orientational order.

Exercise 8.2: Global alignment coefficient. Implement a function that calculates the global alignment coefficient (Eq. 8.5) of a configuration of particles. Test your function on simple cases.

If we want to quantify the level of clustering of a configuration, we can either isolate the clusters one by one, counting the number of particles in each of them, or define a *clustering coefficient* in the following way. Given a configuration, we calculate its *Voronoi tessellation*. A Voronoi tessellation divides the arena in polygonal patches corresponding to each particle so that each patch includes all the points of the arena that are closer to the (only) particle included in the patch than to any other particle (most programming languages provide some built-in functions to calculate it). Given the particle i, let $A_{i,n}$ be the area of the Voronoi polygon for particle i at iteration n. We define the *global clustering coefficient* as:

$$c_n = \frac{\mathrm{count}\left\{A_{i,n} < \pi R_\mathrm{f}^2\right\}}{N}, \tag{8.6}$$

where only particles whose Voronoi cell is smaller than the flocking area are counted. Values of c close to 0 indicate that there are not many clusters. Values of c close to 1 indicate that most particles belong to a cluster, so there is a high level of clustering.

Exercise 8.3: Global clustering coefficient. Implement a function that calculates the global clustering coefficient (Eq. 8.6) of a configuration of particles. Test your function on simple cases.

At this point, we have all the elements to simulate the Vicsek model.

Exercise 8.4: Vicsek model at low noise and low density. In this exercise, take $L = 100$, $N = 100$, $v = 1$, $\Delta t = 1$, $\eta = 0.01$. Implement your code and set the number of iterations to $S = 10^4$ steps. Compare your results with Fig. 8.3.

a. Generate an initial particles' configuration and save it in order to be able to start from exactly the same configuration for different flocking radii R_f. Plot the initial configuration.

b. Perform the simulation for $R_f = 1$. Calculate and plot the global alignment and clustering coefficients as a function of the time step.

c. Plot the configurations after 10, 100, 500, 1000 iterations, and the final configuration.

d. Repeat the simulation starting from the same initial configuration, but taking a larger detection radius (e.g., $R_f = 2, 5, 10, \ldots$).

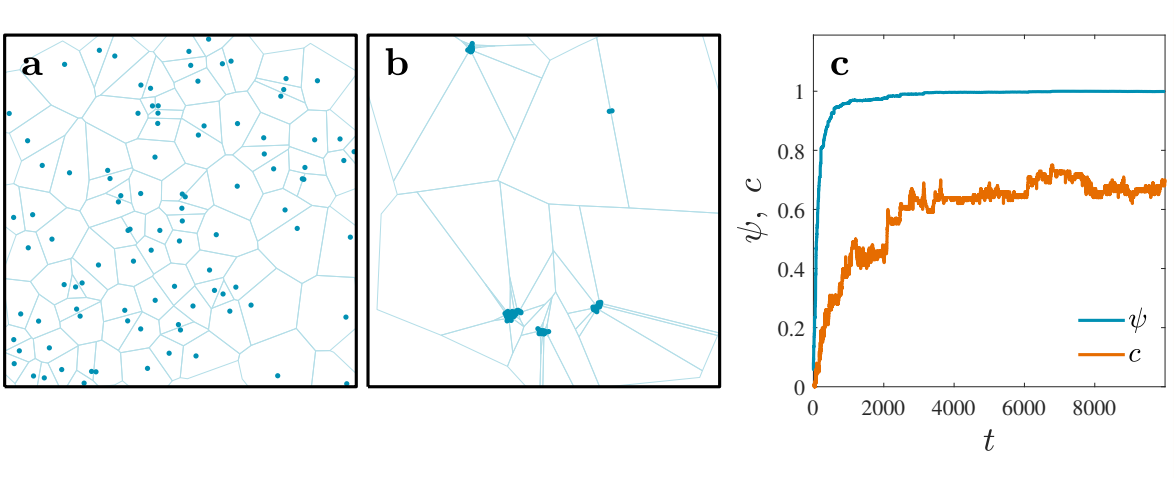

Figure 8.3: **Vicsek model at low noise and low density. a** Initial and **b** final configuration (after 10^4 steps, $N = 100$, $L = 100$, $\eta = 0.01$, $R_f = 1$, $v = 1$). The Voronoi tessellation is outlined by the cyan lines. **c** Global alignment coefficient ψ and global clustering coefficient c as a function of the time step. The global alignment coefficient shows that the particles are aligned after less than 1000 iterations. The clustering coefficients also steadily increases, even though more slowly.

When simulating the Vicsek model at low speed, low densities, and low noise (Exercise 8.4), you should have obtained that the particles organize in small clusters. Fig. 8.3 represents the case for $R_f = 1$. If you repeat the simulation with a different value of R_f, for instance $R_f = 5$, you should notice that the particles, when clustering, tend to remain farther apart from each other. This is due to the aligning mechanism: If R_f is larger, particles start to align with particles further away.

Exercise 8.5: Higher noise. Repeat Exercise 8.4 taking a higher noise level, for example, $\eta = 0.1$. For ease of comparison, maintain the other parameters the same. Run your simulation for $S = 10^4$ steps. Compare your results with Fig. 8.4.

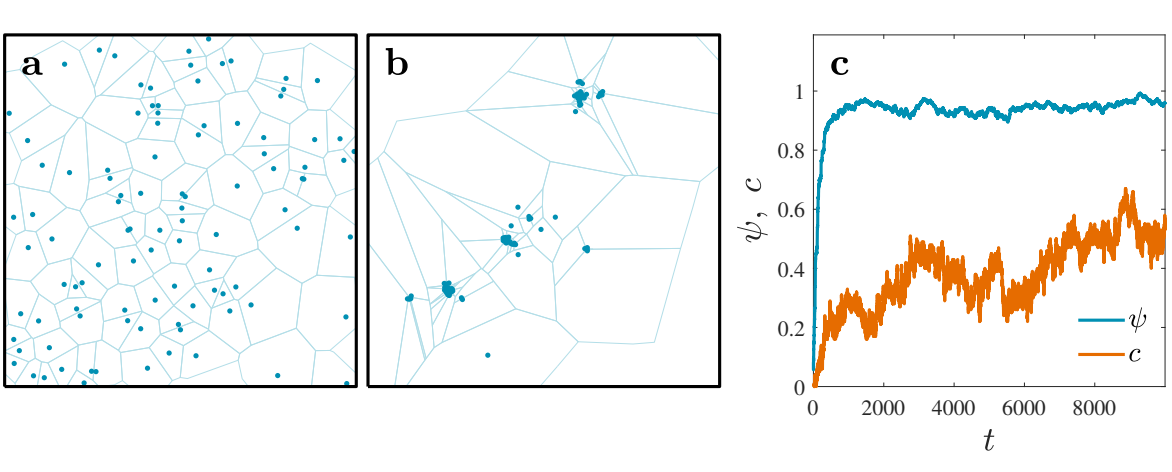

Figure 8.4: **Vicsek model with higher noise.** **a** Initial and **b** final configuration (after 10^4 steps) with the same parameters as in Fig. 8.3, but higher noise ($\eta = 0.1$). **c** Global alignment coefficient ψ and global clustering coefficient c as a function of the time step. Compared to the lower noise case (Fig. 8.3), the global alignment coefficient ψ shows a slightly worse alignment, but it is the clustering coefficient that features the most evident changes demonstrating that the noise makes the clusters smaller and less stable.

Increasing the noise (Exercise 8.5), you can see that the particles are slightly less aligned and slightly worse organized in clusters. If you increase the noise level even more, you should eventually find that the particles are no longer able to align and the clusters become more and more unstable until they cannot form at all.

Exercise 8.6: Higher density. Repeat Exercise 8.4 taking a higher density of particles, for example, $N = 1000$ (keep the other parameters the same). Run your simulation for $S = 10^4$ steps. Compare your results with Fig. 8.5.

Exercise 8.7: Higher density and higher noise. Now repeat Exercise 8.4, increasing both density ($N = 1000$) and noise level ($\eta = 0.1$). Run your simulation and compare your results with Fig. 8.6

Increasing the density (Exercise 8.6), the particles show very soon a phase with a high orientational order. With $R_f = 1$, the particles organize into several stable clusters. If you increase R_f, you will be able to obtain a single giant cluster including all the particles. Increasing the noise level (Exercises 8.7) results in a slightly worse alignment and clustering (Fig. 8.6). If one increases the noise level even more for high density, the particles move in

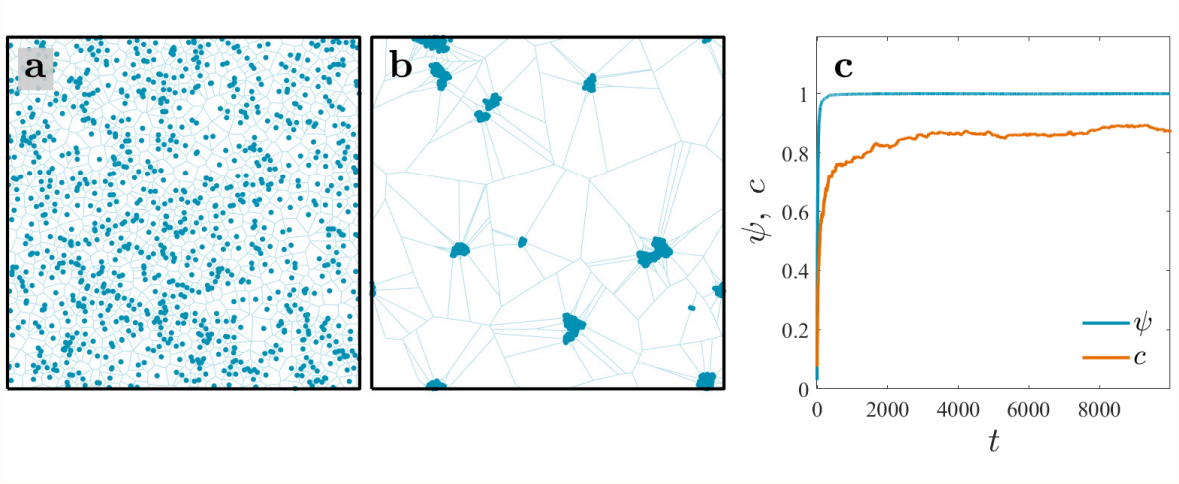

Figure 8.5: **Vicsek model with higher density.** **a** Initial and **b** final configuration (after 10^4 steps) with the same parameters as Fig. 8.3, but higher density ($N = 1000$). **c** Global alignment coefficient ψ and global clustering coefficient c as a function of the time step. Compared to the lower density case (Fig. 8.3), the global alignment coefficient ψ shows a faster and better alignment, and the clustering coefficient c fluctuates less and reaches faster a higher asymptotic value.

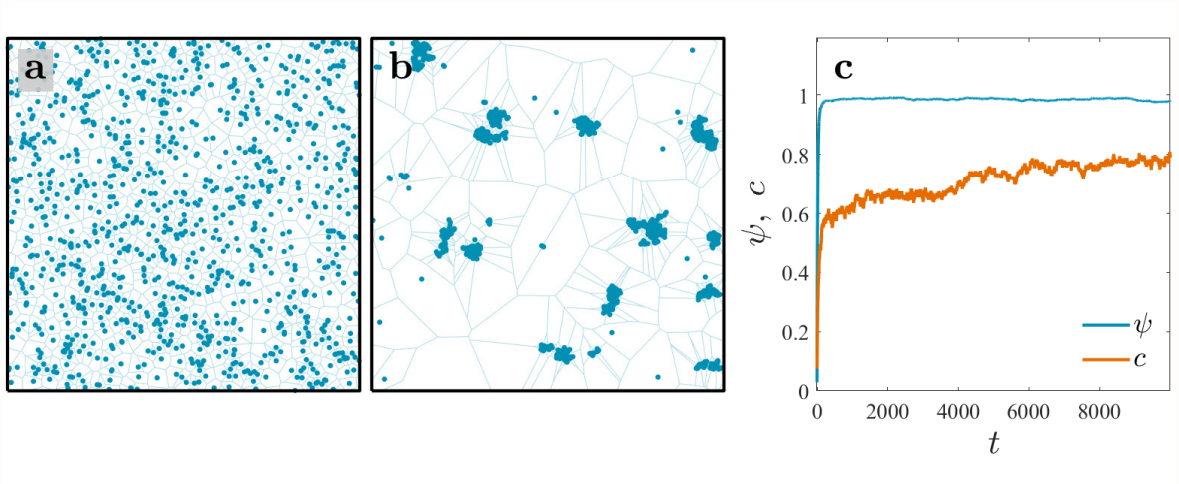

Figure 8.6: **Vicsek model with higher noise and higher density.** **a** Initial and **b** final configuration (after 10^4 steps) with the same parameters as Fig. 8.3, but higher density ($N = 1000$) and higher noise ($\eta = 0.1$). **c** Global alignment coefficient ψ and global clustering coefficient c as a function of the time step. Compared to the case presented in Fig. 8.5 (same density, but lower noise), the global alignment coefficient ψ does not change appreciably, but the clustering coefficient c fluctuates more and reaches a lower value.

an orientationally non-ordered phase, with only some correlation between the directions of nearby particles.

In the previous exercises, we have shown the data obtained from a single, long simulation. To gain insights into the statistical behavior of each of these cases (low density, high density, low noise, high noise), you should repeat the simulations with the same requirements of density and noise level, but different initial conditions, and take the average of the results.

8.2 The effect of delay

Sensory delays might occur when an individual applies rule 8.2 to re-orient itself. In such cases, rule 8.2 becomes

$$\theta_{j,n+1} = \langle \theta_{k,n-h} \rangle + \eta W_n \Delta t \tag{8.7}$$

where the integer h is the delay. If $h = 0$, we have the standard Vicsek model.

Exercise 8.8: Delayed Vicsek model. Take $L = 1000$, $N = 100$, $v = 3$, $\Delta t = 1$, $\eta = 0.4$, $R = 20$, so that the average number of particles within a detection area is not too high ($N_f \approx 0.124$, because at higher density *density waves* might occur — check it out for yourself!). Moreover, the noise is high enough to prevent the formation of stable clusters, but low enough to allow some alignment of the orientation of the particles. With these parameters, the steady state is reached within 5000 time steps (usually much earlier).

a. Generate the initial configuration of positions and orientations. It might be convenient to have the same initial configuration for different values of the delay to ease their comparison.

b. Perform the simulation for $S = 10^4$ time steps for different values of the delay: Take, for example, $h = 0$ (no delay), 1, 2, 3, ..., 25. Check the evolution of the system in each simulation. Compare your results with Fig. 8.7.

c. For each simulation, calculate and plot the global alignment coefficient ψ and the global clustering coefficient c a function of time, comparing the data for different delays h. Compare your result with Fig. 8.8.

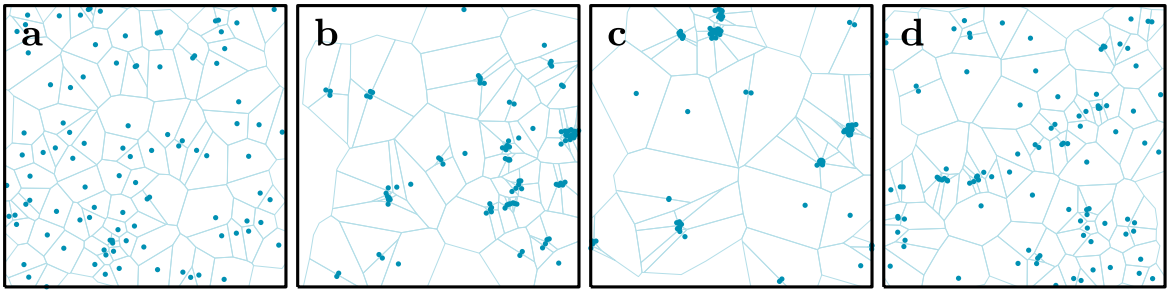

Figure 8.7: **Delayed Vicsek model.** Effect of delay on the Vicsek model ($N = 100$, $L = 1000$, $\eta = 0.4$, $v = 3$). **a** Initial configuration. **b**-**d** Configurations after 1000 iterations for **b** $h = 0$ (no delay), **c** $h = 2$ (short delay, which stabilizes the clustering), and **d** $h = 25$ (long delay, which hinders the clustering).

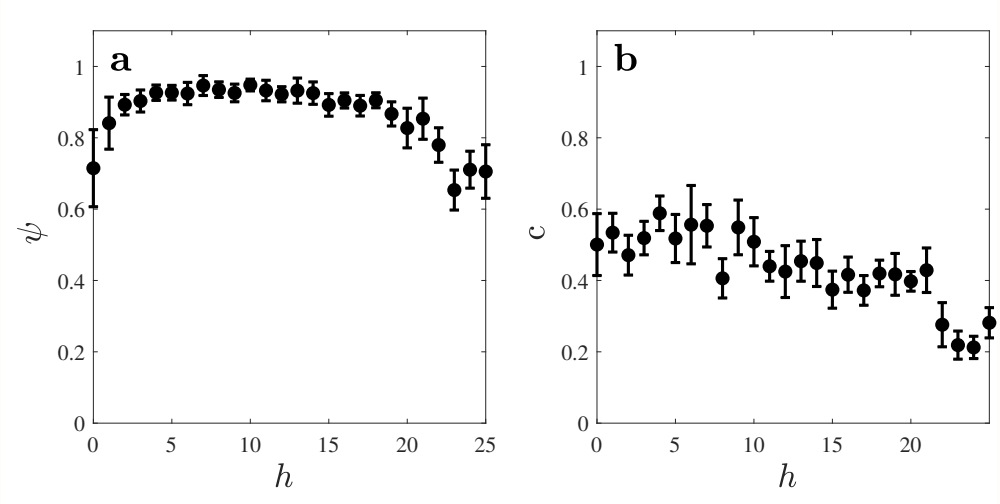

Figure 8.8: **Effect of delay on alignment and clustering.** **a** Global alignment coefficient ψ and **b** global clustering coefficient c as a function of the delay for single simulations (not averaged over different initial conditions). The data points are obtained averaging ψ and c for the configurations after 5000 time steps. The parameters are the same as in Fig. 8.7.

d. Repeat these simulations for various initial conditions and statistically compare the results.

A systematic study of the Vicsek model with delay is provided in Ref. [2], whose results show that the global aligning parameter is not drastically affected by the delay, but the clustering parameter is instead positively affected by the presence of a short delay, while for a longer delay the clustering is hindered.

One can also consider negative delays. We cannot directly use Eq. 8.7, because the expression $\theta_{k,n-h}$, with $h < 0$, refer to the angle at a time step that has not been calculated yet — it is a value in the future, after all. What is the meaning, then, of a negative delay? And how can we understand it? As we will see in Chapter 10, a negative delay can be understood as a prediction: The individual, on the basis of the recent orientation history data, makes a prediction of the future value of the orientation of other individuals within its detection area, and uses this prediction in order to adjust its orientation. It is similar to when you want to move in a crowded place: You give a quick look around, you guess the immediate future trajectory of the other people by evaluating their current position and velocity, and then you decide when and where to move, in order to avoid collisions. Thus, we can use a linear extrapolation of the orientation in the last s time steps to predict the orientation at time $|h|\Delta t$ in the future. As we will see in the following exercise, the presence of a negative delay hinders clusters formation.

Exercise 8.9: Negative delays. Repeat Exercise 8.8 for values of negative delay h between -1 and -15.

a. Implement the procedure that linearly extrapolates the orientation $|h|$ steps into

the future on the basis of the history of the last s orientations of each particle belonging to the detection radius.

b. Run the simulation for a negative delay $h = -1, -2, \ldots, -15$, and compare with the case of no delay ($h = 0$). Treat the case of no delay also with the extrapolation procedure (Is this completely equivalent to the standard Vicsek model? Why?).

c. For each simulation, calculate the global alignment coefficient ψ and the global clustering coefficient c. Compare your results with Fig. 8.9.

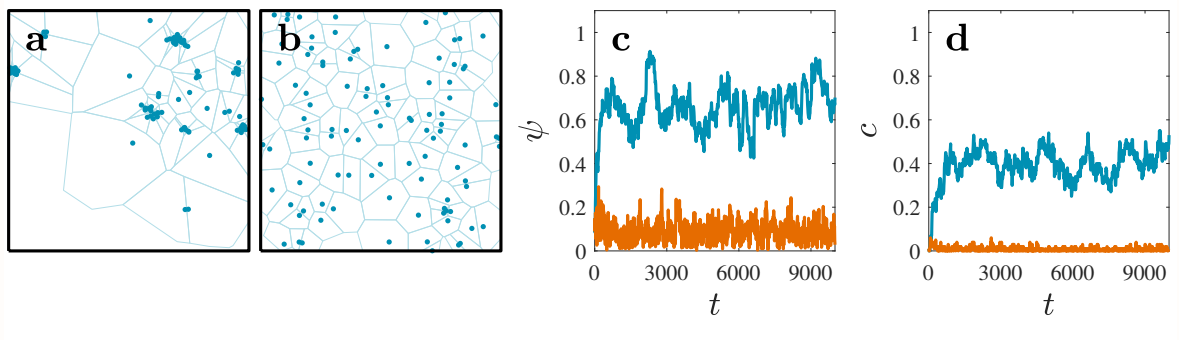

Figure 8.9: **The effect of negative delay.** Final configuration of the Vicsek model with **a** no delay ($h = 0$) and **b** negative delay $h = -2$ (i.e., using the extrapolation of the orientation of the particles two steps into the future). A comparison of the **c** global alignment coefficient ψ and **d** global clustering coefficient c in the two cases (the blue line represents no delay, and the red line represents a negative delay $h = -2$). In the presence of a negative delay, clustering is hindered.

8.3 Non-metric and non-reciprocal interactions

Flocks of birds have been extensively studied to understand whether their interactions follow the rules of the Vicsek model (Eq. 8.2) and, if so, to estimate their interaction radius [3, 4]. Surprisingly, it has been found that birds usually keep into account the orientation of their closest 4 to 8 neighbors, to a large extent independently of their absolute distance, making the interaction *non-metric*. Furthermore, birds outside the field of view might not be seen and, therefore, taken into account, even if they are close by. In these cases, the interaction might turn out to be *non-reciprocal* (e.g., a bird might be influenced by another bird in front of it, but the bird in front is not influenced by the first bird). Therefore, it is interesting to study what happens to the predictions of the Vicsek model in the case of non-metric and non-reciprocal interaction rules. Here, we consider a specific non-metric and non-reciprocal interaction where each individual considers only its k nearest neighbors to decide its orientation in the next step.

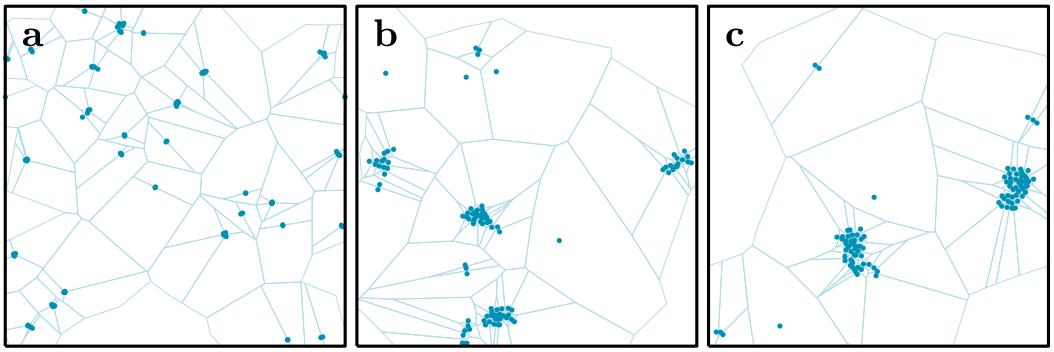

Figure 8.10: **Vicsek model with k nearest neighbors.** Configuration after 10^4 time steps for interactions with only **a** $k = 1$, **b** $k = 4$, and **c** $k = 8$ nearest neighbors ($N = 100$, $L = 100$, $\eta = 0.1$). Note how the size of the clusters increases with the value of k.

Exercise 8.10: Interaction with k nearest neighbors. Repeat Exercise 8.5 by changing the interaction rule. Differently from the standard Vicsek model, calculate the orientation considering only the k nearest neighbors. Try for different values of k (e.g., $k = 1$, 4, 8). Compare your results with Fig. 8.3. Verify that this interaction might be non-metric (i.e., the interaction does not only depend on the metric distance between particles) and non-reciprocal (i.e., if particle j belongs to the k nearest neighbors of particle i, particle i in not necessarily included in the k nearest neighbors of particle j).

Exercise 8.11: Vision cones. Restrict the field of view of the particles in Exercise 8.10 so that they can only see particles in a certain vision cone (e.g., only particles in front of them). Determine how this changes the overall behavior of the system.

8.4 Further readings

The Vicsek model was introduced in Ref. [1]. Its simplicity makes it the ideal benchmark to compare with experimental systems. For example, it has been used in Ref. [5] for experimental investigations of scaling laws in midget swarms and in Ref. [6] to model the information flow in finite active matter flocks as a function of noise. Ref. [7] provides a review of the dynamics and finite-size scaling of the standard Vicsek model. Ref. [8] covers the physics behind the Vicsek model, presenting the results of simulations together with the role played by symmetries and conservation laws.

In the original article [1], it was claimed that the phase transition to a dynamical, collective ordered phase was a continuous (second-order) phase transition. Later, this has been debated, due to the evidence produced by successive numerical simulations that indicated

the phase transition could be discontinuous (first-order) [9]. However, further analysis eventually confirmed the continuous nature of the phase transition [10, 11].

Since delay and imperfect transfer of information may play a crucial role in nature and technology, they must be taken into account to obtain a robust swarming mechanism. For the effect of delay in systems described by the Vicsek model, we refer the reader to Ref. [2]. For applications to describe prey–predator systems, see Ref. [12].

The Vicsek model is not the only model to describe the swarming behavior of self-propelling particles. A more general approach is the Toner–Tu model [13], which includes the Vicsek model as a special case. However, it is of more complex implementation. Other approaches simulate swarming behavior with data-driven approaches [14].

Examples of how experimental studies on real systems are conducted are, for instance, Refs. [15, 16, 3, 4]. Ref. [17] explores theoretical models and empirical studies on collective behavior in animal groups, also discussing its biological aspects. Another interesting reference on collective behavior is Ref [18].

Bibliography

[1] T. Vicsek, A. Czirók, E. Ben-Jacob, I. Cohen, and O. Shochet. Novel type of phase transition in a system of self-driven particles. *Phys. Rev. Lett.*, 75:1226, 1995.

[2] R. Piwowarczyk, M. Selin, T. Ihle, and G. Volpe. Influence of sensorial delay on clustering and swarming. *Phys. Rev. E*, 100:012607, 2019.

[3] M. Ballerini, N. Cabibbo, R. Candelier, A. Cavagna, E. Cisbani, I. Giardina, V. Lecomte, A. Orlandi, G. Parisi, A. Procaccini, M. Viale, and V. Zdravkovic. Interaction ruling animal collective behavior depends on topological rather than metric distance: Evidence from a field study. *PNAS*, 105:1232, 2008.

[4] A. Cavagna, A. Cimarelli, I. Giardina, G. Parisi, R. Santagati, F. Stefanini, and R. Tavarone. From empirical data to inter-individual interactions: unveiling the rules of collective animal behavior. *Math. Models Methods Appl. Sci.*, 20:1491, 2010.

[5] A. Cavagna, D. Conti, C. Creato, L. Del Castello, I. Giardina, T. S. Grigera, S. Melillo, L. Parisi, and M. Viale. Dynamic scaling in natural swarms. *Nat. Phys.*, 13:914, 2017.

[6] J. Brown, T. Bossomaier, and L. Barnett. Information flow in finite flocks. *Sci. Rep.*, 10:3837, 2020.

[7] G. Baglietto, E. V. Albano, and J. Candia. Criticality and the onset of ordering in the standard Vicsek model. *Interface Focus*, 2:708, 2012.

[8] F. Ginelli. The physics of the Vicsek model. *Eur. Phys. J. Spec. Top.*, 225:2099, 2016.

[9] G. Grégoire and H. Chaté. Onset of collective and cohesive motion. *Phys. Rev. Lett.*, 92:025702, 2004.

[10] M. Nagy, I. Daruka, and T. Vicsek. New aspects of the continuous phase transition in the scalar noise model (snm) of collective motion. *Phys. A: Stat. Mech. Appl.*, 373:445, 2007.

[11] M. Aldana, H. Larralde, and B. Vázquéz. On the emergence of collective order in swarming systems: a recent debate. *Int. J. Mod. Phys. B*, 23:3661, 2009.

[12] S. Mohapatra and P. S. Mahapatra. Confined system analysis of a predator-prey minimalistic model. *Sci. Rep.*, 9:11258, 2019.

[13] J. Toner and Y. Tu. Long-range order in a two-dimensional dynamical XY model: How birds fly together. *Phys. Rev. Lett.*, 75:4326, 1995.

[14] J. Ren, X. Wang, X. Jin, and D. Manocha. Simulating flying insects using dynamics and data-driven noise modeling to generate diverse collective behaviors. *PLoS One*, 11:1, 2016.

[15] M. Nagy, Z. Akos, D. Biro, and T. Vicsek. Hierarchical group dynamics in pigeon flocks. *Nature*, 464:890, 2010.

[16] G. Ariel and A. Ayali. Locust collective motion and its modeling. *PLoS Comput. Biol.*, 11:e1004522, 2015.

[17] I. Giardina. Collective behavior in animal groups: Theoretical models and empirical studies. *HFSP J.*, 2:205, 2008.

[18] T. Vicsek and A. Zafeiris. Collective motion. *Phys. Rep.*, 517:71, 2012.

[19] A. Czirók, M. Vicsek, and T. Vicsek. Collective motion of organisms in three dimensions. *Phys. A: Stat. Mech. Appl.*, 264:299, 1999.

[20] B. Gönci, M. Nagy, and T. Vicsek. Phase transition in the scalar noise model of collective motion in three dimensions. *Eur. Phys. J. Spec. Top.*, 157:53, 2008.

[21] R. Soto and R. Golestanian. Self-assembly of active colloidal molecules with dynamic function. *Phys. Rev. E*, 91:052304, 2015.